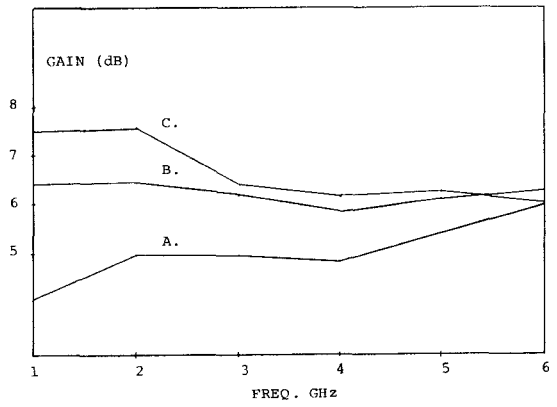


Fig. 8. Measured performance of chip $S/N$ 001. Three curves are for different values of $R_F$. ($A$: $R_F = 241$; $B$: $R_F = 366\ \Omega$; $C$: $R_F = 491\ \Omega$.).

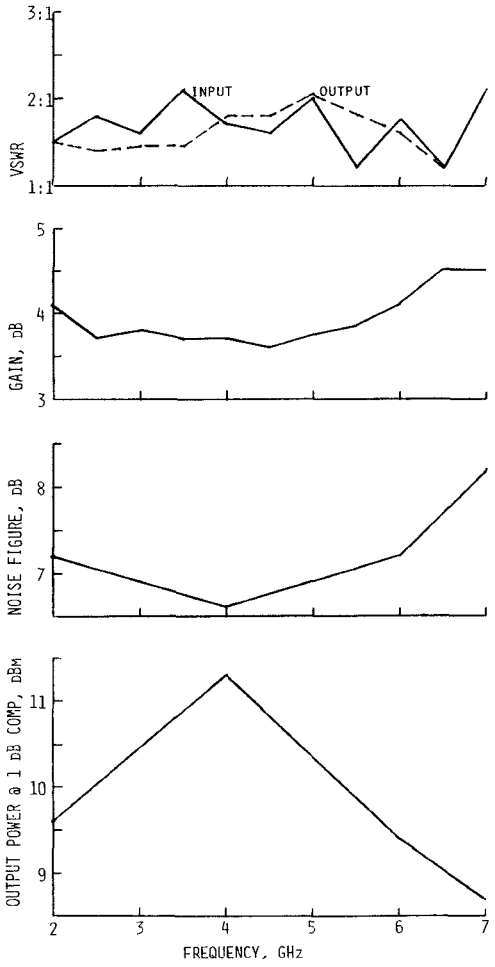


Fig. 9 Measured performance of $S/N$ 002.

## IX. Performance

The monolithic circuit was bonded into an alumina hybrid test fixture consisting of input and output 50-Ω microstrip lines with lumped-element bias networks. Gain performance from 1 to 6 GHz using various values of feedback resistance are shown in Fig. 8. As expected, the gain is improved with high values of feedback resistance at the expense of VSWR's and gain flatness. The optimum value of resistance (350 Ω) is substantially higher than expected and is presently being attributed to the excessive series resistance of the inductors. It is also believed that chip to chip variations and lower than predicted gain are the result of inconsistent gold plating in the inductors.

The noise figure and output power of a second amplifier chip was measured in the 2–7-GHz band and is shown in Fig. 9. We believe the noise figure can be reduced by another 2 dB by eliminating the losses in the input inductor.

## X. Conclusion

The use of feedback techniques has been employed to realize monolithic amplifier chips in the 1–7-GHz band. Spiral inductors, interdigital capacitors, and thin film metal resistors were developed and integrated with self-aligned gate FET's to achieve 6-dB gain across this band.

Further work will center on the reduction of inductor loss and the integration of bias filter elements to improve gain and noise figure, and to reduce the size and cost of final amplifier assemblies.

## Acknowledgment

The authors wish to thank J. Eisenberg, D. Strange, S. Ali, and R. Hamilton for their help in designing, processing, and testing these amplifiers.

## References

[1] I. F. Perez and V. Ortega, "A graphical method for the design of feedback networks for microwave transistor amplifiers: Theory and applications," *IEEE Trans. Microwave Theory Tech.*, vol. MTT-29, Oct. 1981.

[2] K B. Niclas, "GaAs MESFET feedback amplifiers, design considerations and characteristics," *Microwave J.*, vol. 23, No. 3, Mar. 1980.

[3] P. A. Terzian, R. D. Fairman, and M. M. Nowak, "Self-alignment yields submicron gates for FETs," *Microwave Systems News*, vol. 7, No. 2, Feb. 1977.

[4] Y. C. Lim and R. A. Moore, "Properties of alternately charged coplanar parallel strips by conformal mapping," *IEEE Trans. Electron Devices*, vol. ED-15, pp. 173–180, Mar. 1968.

[5] F. W. Grover, *Inductance Calculations: Working Formulas and Tables*. New York: Dover, 1946.

[6] J. S. Joshi, J. R. Cockrill, and J. A. Turner, "Monolithic microwave gallium arsenide FET oscillators," *IEEE Trans Electron Devices*, vol. ED-28, Feb. 1981.

# Slow Waves Guided by Parallel Plane Tape Guides

HERMAN J. FINK AND JOHN R. WHINNERY, FELLOW, IEEE

***Abstract*—Waves guided by two parallel metallic plates of infinite extent, containing cuts at periodic intervals, are investigated for a number of cases with special emphasis upon the relative directions of the cuts in the top and bottom plates. Two fundamental slow-wave modes exist for all frequencies, in general. The latter are functions of tilt angles of the cuts, frequency, and plate separation. For tilt angles $\Psi$ in the top and $\pm\Psi$ in the**

Manuscript received March 23, 1982; revised May 4, 1982.

H. J. Fink is with the Department of Electrical and Computer Engineering, University of California, Davis, CA 95616.

J. R. Whinnery is with the Department of Electrical Engineering and Computer Science, University of California, Berkeley, CA 94720.

**bottom plane, the amplitudes of the even and odd modes are independent of each other, while for other angles in the bottom plane a predetermined linear combination of even and odd terms exist for each mode.**

Helical wires or tapes have been useful as antennas [1] or slow-wave structures for interaction with an electron beam in traveling-wave tubes [2]. The sheath-helix model assumes a cylindrical surface of radius $r$ which is perfectly conducting in the direction of the helical wire or tape, and perfectly insulating for directions normal to the latter direction. This model was introduced for the purpose of analyzing waves on periodic structures by Pocklington [3] and later by Ollendorf [4] and is described in standard texts [2], [5]. Results give good predictions of propagation behavior for the fundamental wave, although higher order space harmonics require knowledge of the period and dimensions of wire or tape. Planar equivalents of the circular cylindrical sheath helix are of interest pedagogically [6]. There is also an advantage sometimes in using a slab electron beam for interaction with the slow-wave structure to permit a larger fraction of the beam to be near the periodic structure. Analysis for such a structure has been given for a particular propagation direction [7], but there are some interesting questions relating to the direction of wavefronts with respect to the cuts. These are examined with attention to current and power flow. The situation is clearly related to that of surface waves along single unidirectionally conducting planes that have been extensively studied [8]–[10], and in certain cases the double plane modes which may be considered a coupling of surface waves propagating along the two individual planes.

We are considering a guide consisting of two metallic plates parallel to the $(zy)$-plane and separated a distance $2a$ along the $x$-direction, (Fig. 1). The width of the metallic plates along the $y$-direction is assumed to be very much larger than $2a$ so that spatial variations of the electric ($E$) and magnetic ($H$) fields with $y$ can be neglected. Boundary conditions at $y = \pm\infty$ will be discussed separately for the different cases considered. Slots are cut into the plates, inclined by some angle $\Psi$ with respect to the $y$-direction on the top and $\delta$ on the bottom. In the sheath model the slot spacings are infinitesimal. The guide then approximates a parallel plane "tape guide". We assume that a single frequency wave is propagating parallel to the $z$-direction and the electric (and magnetic fields) are of the form

$$\boldsymbol{E}(x,z,t) = \boldsymbol{E}(x)\,e^{j(\omega t-\beta z)} \tag{1}$$

where $\omega$ is the radian frequency and $\beta$ the phase constant. The latter is related to the propagation constant $\gamma$ by $\gamma = \alpha + j\beta$. The space between and outside the plates is filled with the same loss-free material. The reduced wave equation

$$\frac{\partial^2 \boldsymbol{E}}{\partial x^2} = (\beta^2 - k^2)\boldsymbol{E} \equiv \tau^2 \boldsymbol{E} \tag{2}$$

then gives wave types of the following form.

*For* $-a \leqslant x \leqslant a$ (*medium* 1):

$$E_{z1} = (A_1 \cosh\tau x + B_1 \sinh\tau x)\,e^{j(\omega t-\beta z)} \tag{3}$$

$$H_{z1} = (C_1 \cosh\tau x + D_1 \sinh\tau x)\,e^{j(\omega t-\beta z)}. \tag{4}$$

*For* $|x| \geqslant a$ (*medium* 2):

$$E_{z2} = (A_2 e^{-\tau x} + B_2 e^{\tau x})\,e^{j(\omega t-\beta z)} \tag{5}$$

$$H_{z2} = (C_2 e^{-\tau x} + D_2 e^{\tau x})\,e^{j(\omega t-\beta z)}. \tag{6}$$

For a confined solution we must have $\tau > 0$ and $B_2 = D_2 = 0$ for $x \geqslant a$ and $A_2 = C_2 = 0$ for $x \leqslant -a$. There are 8 constants of integration, $A_1, B_1, \cdots, D_2$ and the unknown eigenvalue $\tau = +\sqrt{\beta^2 - k^2}$, where $k = \omega/v$, $\beta = \omega/v_p$, $v = 1/\sqrt{\mu\epsilon}$, and $v_p$ is the phase velocity of the wave. Furthermore, $E_y$, $H_y$, $E_x$, and $H_x$ are obtained from

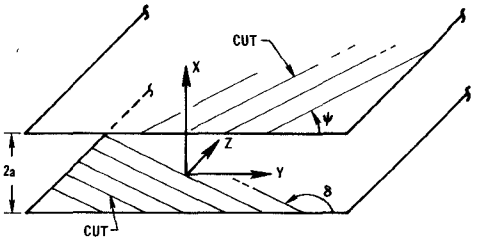


Fig. 1. Model of parallel-plane tape guide discussed in the text.

$$E_{y1,2} = -j\frac{k\eta}{\tau^2}\frac{\partial H_{z1,2}}{\partial x} = -\frac{k\eta}{\beta}H_{x1,2} \tag{7}$$

$$H_{y1,2} = j\frac{k}{\tau^2\eta}\frac{\partial E_{z1,2}}{\partial x} = \frac{k}{\beta\eta}E_{x1,2} \tag{8}$$

where $\eta = \sqrt{\mu/\epsilon}$ is the intrinsic impedance. In order to obtain the constants of integration and the eigenvalue $\tau$ we have to apply boundary conditions at $x = \pm a$. We assume that the anisotropic sheath boundary conditions apply. These are:

1) The current in the metallic tape is finite; the conductivity parallel to the tape $\sigma_{//}$ is assumed to be infinite so that $E_{//1} = E_{//2} = 0$.
2) There is no current perpendicular to the tape so we must have $E_{\perp 1} = E_{\perp 2}$.
3) Because there is no current perpendicular to the tape we must also have $H_{//1} = H_{//2}$.

We consider now three distinct cases which we shall compare with each other (see Fig. 1).

*Case 1):* The tape is inclined by an angle $\Psi$ with respect to the $y$-direction both in the top and bottom planes.

*Case 2):* The tape is inclined by an angle $\Psi$ in the top plane and an angle $(180° - \Psi)$ in the bottom plane with respect to the $y$-direction (or $-\Psi$).

*Case 3):* The tape is inclined by an angle $\Psi$ in the top plane and an angle $(90° + \Psi)$ in the bottom plane with respect to the $y$-direction.

The general boundary conditions at $x = \pm a$ are, where $\Psi$ is defined for $x = +a$ and $\delta$ for $x = -a$

$$E_{z1}\sin\left(\frac{\Psi}{\delta}\right) + E_{y1}\cos\left(\frac{\Psi}{\delta}\right) = 0 \tag{9}$$

$$E_{z2}\sin\left(\frac{\Psi}{\delta}\right) + E_{y2}\cos\left(\frac{\Psi}{\delta}\right) = 0. \tag{10}$$

$$E_{z1}\cos\left(\frac{\Psi}{\delta}\right) - E_{y1}\sin\left(\frac{\Psi}{\delta}\right) = E_{z2}\cos\left(\frac{\Psi}{\delta}\right) - E_{y2}\sin\left(\frac{\Psi}{\delta}\right) \tag{11}$$

$$H_{z1}\sin\left(\frac{\Psi}{\delta}\right) + H_{y1}\cos\left(\frac{\Psi}{\delta}\right) = H_{z2}\sin\left(\frac{\Psi}{\delta}\right) + H_{y2}\cos\left(\frac{\Psi}{\delta}\right). \tag{12}$$

*Case 1):* For $\delta = \Psi$, (9)–(12) lead to

$$A_1\left(1 - \left(\frac{\tau}{k}\tan\Psi\right)^2\right) = 0 \tag{13}$$

$$B_1\left(1 - \left(\frac{\tau}{k}\tan\Psi\right)^2\right) = 0. \tag{14}$$

We therefore have two modes with arbitrary amplitudes $A_1$ and $B_1$, the first of which has an $E_{z1}$ component which is even in the spatial coordinate $x$, the second is odd in $x$. Both modes have the

same eigenvalue

$$\tau = k\cot\Psi \tag{15}$$

and phase and group velocities

$$v_p = v_g = v\sin\Psi. \tag{16}$$

The complete solution is then a linear superposition of the two independent modes with the same phase constant $\beta$.

There are several interesting points concerning these results. First note, as in the surface waves along single planes, that when wavefronts are normal to the cuts $\Psi = \pi/2$, $\tau = 0$, and the wave reduces just to the TEM wave between parallel planes. This is expected since the cuts are along the current flow lines of this mode. For other $\Psi$, we note that current flow for the mode with $E_z$ odd in $x$ ($A_1 = 0$, $B_1 \neq 0$) flows in opposite directions in top and bottom conductors since surface current density is $\hat{x} \times \boldsymbol{H}$ in the bottom, $-\hat{x} \times \boldsymbol{H}$ in the top. Conductors could thus be connected at $y = \pm\infty$ to supply the current return. For the mode with $E_z$ even in $x$, current flow is in the same direction in top and bottom, so something other than direct connection at the edges is necessary for such modes. The average Poynting vector has components in the $y$ and $z$ directions which are related by

$$\frac{P_{z1}}{P_{y1}} = \frac{k}{\tau} = \tan\Psi$$

for both even and odd modes. Thus, power flow is along the wires in Case 1) for all modes and all orientations of wavefronts with respect to the cuts. This is of course a consequence of the constraint on the direction of the current flow.

*Case 2):* The case of $\delta = 180° - \Psi$ is that analyzed in [7]. We wish to include this for comparison with other cases:

$$A_1\left(1 - \left(\frac{\tau}{k}\tan\Psi\right)^2 \coth\tau a\right) = 0 \tag{17}$$

$$B_1\left(1 - \left(\frac{\tau}{k}\tan\Psi\right)^2 \tanh\tau a\right) = 0. \tag{18}$$

Assuming that $\omega$, $\Psi$, $\mu\epsilon$, and $a$ are fixed, there exist two different modes with independent and arbitrary amplitudes $A_1$ and $B_1$ and with different eigenvalues $\tau_1$ and $\tau_2$, given by

$$\tau_1^2 \coth\tau_1 a = \tau_2^2 \tanh\tau_2 a = k^2\cot^2\Psi. \tag{19}$$

Each mode then has a different phase constant and phase velocity, a plot of the latter as a function of $2a/\lambda$ ($\lambda$ = wavelength in unbounded medium) is shown in Fig. 2 for various values of $\Psi$. The general solution is then a linear combination of the two independent modes with different phase constants, e.g.,

$$E_{z1} = A_1(\cosh\tau_1 x)\, e^{j(\omega t - \beta_1 z)} + B_1(\sinh\tau_2 x)\, e^{j(\omega t - \beta_2 z)}.$$

Unlike Case 1), the mode with $E_z$ even in $x$ ($A_1 \neq 0$, $B_1 = 0$) has equal and opposite $y$-directed surface current densities in the top and bottom tapes, so the edges may be connected at $y = \pm\infty$ to provide the current return path. This case is much like a rectangular tape helix. The mode with $E_z$ odd in $x$ ($A_1 = 0$, $B_1 \neq 0$) has equal current densities in the same $y$-direction in both the top and bottom tape. Therefore, separate current return paths are required as discussed in Case 1).

The average Poynting vector in the $y$-direction is an odd function of $x$ in this case for both the even- and odd-mode types. The $z$-component is even, but it is zero on the central plane for the modes with $E_z$ even in $x$, and nonzero for those with $E_z$ odd. The total power, integrated over the cross section, is finite in the $z$-direction, as pointed out in [7], but zero in the $y$-direction. However, there is nevertheless transverse power flow in the $y$-direction in opposite directions in top and bottom regions.

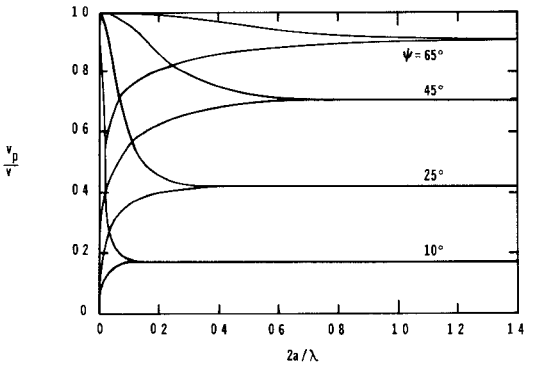


Fig. 2. The phase velocity is plotted as a function of $2a/\lambda$ for Case 2), where $2a$ is the separation of the plates and $\lambda$ the wavelength in the unbounded medium. For $A_1 = 0$ and $B_1 \neq 0$, the value of $v_p \to v$ for $2a/\lambda \to 0$, and for $A_1 \neq 0$ and $B_1 = 0$, $v_p \to 0$ in the same limit

*Case 3):* For more general angles, there is not a simple separation between even and odd modes. We illustrate this for the case of cuts in top and bottom at right angles $\delta = 90° + \Psi$. Equations (9) through (12) then lead to the eigenvalue equation

$$\left(\left(\frac{k}{\tau}\right)^2 - \coth\tau a\right)\left(\left(\frac{k}{\tau}\right)^2 - \tanh\tau a\right) = \left(1 + \left(\frac{k}{\tau}\right)^2\right)^2 \cos^2 2\Psi \tag{20}$$

and to

$$\frac{B_1}{A_1} = \cos 2\Psi \frac{1 + (k/\tau)^2}{\tanh\tau a - (k/\tau)^2} \qquad (\Psi \neq 45°). \tag{21}$$

Provided that $\omega$, $\Psi$, $\mu\epsilon$, and $a$ are fixed, the eigenvalue equation leads to two values of $\tau > 0$, namely $\tau_1$ and $\tau_2$, thus to two independent modes with different phase velocities and phase constants. However, the ratio between the spatially odd and even components of $E_{z1}(x)$ is fixed now. Both must be present for a slow wave to propagate in this structure. Figs. 3 and 4 show $v_p/v$ and $B_1/A_1$ (plus sign for $\Psi < 45°$ and minus sign for $\Psi > 45°$) as a function of $2a/\lambda$ for various angles $\Psi$. The complete solution is then a superposition of the two modes, e.g.,

$$E_{z1} = E_{z1}(\tau_1) + E_{z1}(\tau_2)$$

where

$$E_{z1}(\tau_1) = A_1\left(\cosh\tau_1 x + \frac{B_1}{A_1}\sinh\tau_1 x\right) e^{j(\omega t - \beta_1 z)}$$

with $A_1$ arbitrary and $B_1/A_1$ determined for given values of $\Psi$ and $2a/\lambda$. A similar equation exists for $E_{z1}(\tau_2)$ with the premultiplier in front of the parenthesis arbitrary and the rest determined. Thus, in this case we have again two independent modes with different phase velocities and arbitrary amplitudes, but each mode contains a predetermined linear combination of spatially $x$-dependent even and odd terms.

For this latter case we find that the surface current densities in the top and bottom planes are unequal, in general, for a given value of $z$ (except for $\Psi = 45°$ when Case 3) reduces to Case 2)). The phasor currents per unit length (perpendicular to the current flow) for each mode ($\tau_1$ and $\tau_2$) are (with propagation factors understood)

$$\overrightarrow{J(a)} = -j\frac{k}{\tau}\frac{1}{\eta}\frac{e^{\tau a}}{\sin\Psi}A_1\left(1 + \frac{B_1}{A_1}\right)(\hat{z}\sin\Psi + \hat{y}\cos\Psi) \tag{22}$$

$$\overrightarrow{J(-a)} = -j\frac{k}{\tau}\frac{1}{\eta}\frac{e^{\tau a}}{\cos\Psi}A_1\left(1 - \frac{B_1}{A_1}\right)(\hat{z}\cos\Psi - \hat{y}\sin\Psi). \tag{23}$$

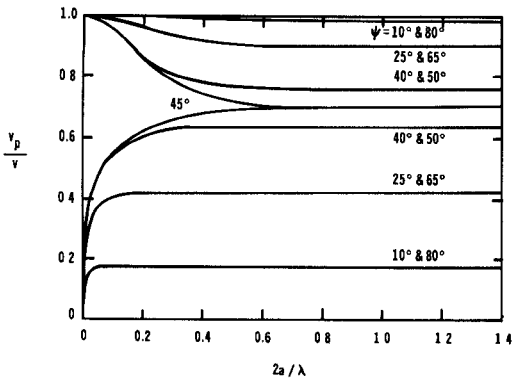


Fig. 3. The same as Fig. 2 except for Case 3). The ratio $B_1/A_1$ is now determined by the guide parameters.

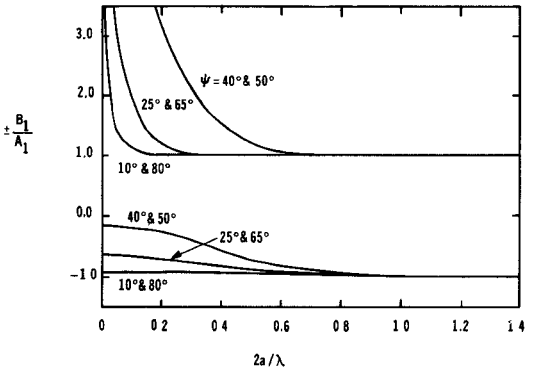


Fig. 4. The ratio $B_1/A_1$ is plotted as a function of $2a/\lambda$ corresponding to Fig. 3. Plus sign for $\Psi < 45°$, minus for $\Psi > 45°$.

In general, external current return paths at $y = \pm\infty$ are necessary as for one of the two modes for Cases 1) and 2).

The Poynting vectors $P_{z1}$ and $P_{y1}$ are in general ($\Psi \neq 45°$) a linear combination of odd and even functions in $x$. The wave front is always perpendicular to the $z$-direction. Neither the spatial integral over area $xy$ of $P_{z1}$ nor that over area $xz$ of $P_{y1}$ is zero in general. The latter is different from Case 2). In the limit that $2a \gtrsim \lambda$, the power flow ratio connected with the lower branch in Fig. 3 ($0 < \Psi < 45°$) is

$$P_{z1}/P_{y1} = \tan\Psi$$

while that connected with the upper branch ($0 < \Psi < 45°$) is

$$P_{z1}/P_{y1} = \tan(\Psi + 90°).$$

In that limit, the power flow connected with the lower branch flows along the slots of the top plate and its power density falls off exponentially from it toward the other plate while the power flow connected with the mode of the upper branch flows along the slots in the bottom plate and its density falls off exponentially toward the top plate. When $2a < \lambda$, these two surface-like modes become more strongly affected by the boundary conditions on the opposite plate and the Poynting vector for each mode is rotated away from the directions of the slots.

## Discussion and Conclusion

All three cases have two slow-wave modes. For Case 1), the phase velocity of the two modes is the same and independent of $2a/\lambda$. In principle, they exist for all frequencies within the context of the anisotropic sheath model. For Cases 2) and 3), each mode has, in general, a different phase velocity at a given frequency. For both cases, $v_p/v \to 1$ for one mode and $v_p/v \to 0$ for the other mode when the signal frequency approaches zero. For wavelengths smaller than the separation of the two anisotropic sheaths of the guide, the phase velocities become frequency independent. In Case 2) they approach each other, while in Case 3) they stay separated, except for $\Psi = 45°$, in which instant Case 3) reduces to Case 2). Thus, for Case 3) there are regions of phase velocities for which neither of the two modes can propagate at any frequency ($\Psi \neq 45°$), and the separate modes remain distinct even at high frequencies. Within the present model all phase velocities in the above structures are smaller than $v$ except for $\lambda \to \infty$ where for one of the modes of Cases 2) and 3), $v_p \to v$.

It is important to realize that when the $y$-axis is not bisecting the angle between the top and bottom slots ($\delta \neq \Psi$) that the wavefront is perpendicular to the $z$-direction and propagating along it while the Poynting vector for each mode is along the slots for $2a \gtrsim \lambda$ and the wave is of a surface-like nature. The mode of the upper branch in Fig. 3 clings to the bottom plate while the lower branch clings to the top plate ($0 < \Psi < 45°$). Each mode is a linear combination of spatially odd and even terms whose amplitude ratio is fixed by the angles $\delta$ and $\Psi$.

One of the two mode types of Cases 1) and 2) and the single modes in Case 3) ($\Psi \neq 45°$) require at $y = \pm\infty$ current returns which are something other than just direct connection at the edges.

## References

[1] J. D. Kraus, *Antennas*. New York: McGraw-Hill, 1950, ch. 7.
[2] J. R. Pierce, *Traveling-Wave Tubes*. New York: Van Nostrand, 1950, ch. 3 and Appendix II.
[3] H. C. Pocklington, Electrical Oscillations in Wires, in *Proc. Camb. Phil. Soc.*, vol. 9, p. 324, 1897.
[4] F. Ollendorf, *Die Grundlagen der Hochfrequenztechnik*. Berlin: Springer, 1926, p. 79.
[5] S. Ramo, J. R. Whinnery, and T. Van Duzer, *Fields and Waves in Communication Electronics*. New York: Wiley, 1965, sec. 8.17.
[6] _____, *Fields and Waves in Communication Electronics*. New York: Wiley, 1965, problem 8.17a.
[7] R. K. Arora, "Surface waves on a pair of parallel unidirectionally conducting screens," *IEEE Trans. Antennas Propagat*, vol. AP-14, p. 795, 1966.
[8] V. H. Rumsey, "A new way of solving Maxwell's equations," *IRE Trans. Antennas Propagat.*, vol. AP-9, pp. 461–465, 1961.
[9] F. C. Karal and S. N. Karp, "Excitation of surface waves on a unidirectional conducting screen by a phased line source," *IEEE Trans. Antennas Propagat.*, vol. AP-12, pp. 470–478, 1964.
[10] L. B. Felsen and H. Hessel, "Radiation and guiding in the presence of a unidirectionally conducting screen," *IEEE Trans. Antennas Propagat*, AP-14, pp. 62–72, 1966.

# A Method to Generate Conservation Laws for Coupled Transmission Systems

O. SCHWELB, MEMBER, IEEE

***Abstract*—A systematic method is presented for generating a set of conservation laws for spatially distributed coupled linear systems. In contrast with previous practice, where energy balance equations were obtained by manipulating the fundamental equations of the interaction (the Maxwell equations or the equations of mechanics), or by determining the invariant**

Manuscript received October 12, 1981; revised June 22, 1982. This work was supported in part by the Natural Sciences and Engineering Research Council, Canada.

The author is with the Department of Electrical Engineering, Concordia University, Montreal, Quebec, H3G 1M8.

0018-9480/82/1100-2023$00.75 ©1982 IEEE